

# Improvement of Classification Accuracy of Four-Class Voluntary-Imagery fNIRS Signals using Convolutional Neural Networks

**Md. Mahmudul Haque Milu**

Department of Biomedical Engineering, Jashore University of Science and Technology (JUST), Bangladesh  
mahmudhmilu@gmail.com

**Md. Asadur Rahman**

Department of Biomedical Engineering, Military Institute of Science and Technology (MIST), Bangladesh  
bmeasadur@gmail.com

**Mohd Abdur Rashid**

Department of EEE, Noakhali Science and Technology University, Bangladesh | Division of Electronics and Informatics, Gunma University, Japan  
marashid.eee@nstu.edu.bd  
(corresponding author)

**Anna Kuwana**

Division of Electronics and Informatics, Gunma University, Japan  
kuwana.anna@gunma-u.ac.jp

**Haruo Kobayashi**

Division of Electronics and Informatics, Gunma University, Japan  
koba@gunma-u.ac.jp

*Received: 23 January 2023 | Revised: 6 February 2023 | Accepted: 8 February 2023*

## ABSTRACT

Multiclass functional Near-Infrared Spectroscopy (fNIRS) signal classification has become a convenient way for optical brain-computer interface. fNIRS signal classification with high accuracy is a challenging assignment while the signals are produced by means of voluntary and imagery movements of the same limb. Since the activation in time and space of voluntary and imagery movement show a similar pattern, the classification accuracy by the conventional shallow classifiers cannot reach an acceptable range. This paper proposes an accuracy improvement approach with the use of Convolutional Neural Networks (CNNs). In this work, voluntary and imagery hand movements (left hand and right hand) were performed by several participants. These four-class signals were acquired utilizing fNIRS devices. The signals were separated based on the tasks and filtered. With manual feature extraction, the signals were classified by support vector machine and linear discriminant analysis. The automatic feature extraction and classification mechanism of the CNN were applied to the fNIRS signals. From the results, it was found that CNN improves the classification accuracy to an acceptable range, which has not been achieved by any convolutional network.

*Keywords-fNIRS; voluntary and imagery fNIRS signal; classification accuracy; conventional classifiers; Convolutional Neural Network (CNN)*

## I. INTRODUCTION

Brain-Computer Interface (BCI) is a remarkable notion of current neuro-computational research that offers the scope to

control the computer with brain commands. Research and development regarding BCI can strongly contribute to neuro-prosthetics applications [1-2]. A brain-controlled computer needs to read the brain functionalities properly. The brain

functionalities can be assessed by both invasive and non-invasive procedures with non-invasive procedures being the primary choice of modern BCI [3]. Electroencephalography (EEG) and magneto-encephalography (MEG) are well-known noninvasive methods based on electric impulsive signals of the brain. Due to some questionable features like noise sensitivity, poor spatial resolution, and motion sensitivity, these modalities should be replaced by some newer ones [4-5].

To meet the challenge of overcoming the previous limitations, functional Near-Infrared Spectroscopy (fNIRS) is a widely used noninvasive optical modality that can measure functional neuro-activations based on the hemodynamics of the brain tissue [6-7]. Although this modality is comparatively slower than the EEG and MEG regarding the brain response, due to very high spatial resolution and robust activation level, fNIRS gets significant importance in BCI research and applications [8-10]. For BCI the brain is to be stimulated externally or internally, with procedures termed as stimuli. Most of the stimuli are provided to the brain in BCI research by imagery or voluntary motor actions [11]. These movement-related functions of the brain correlate with the motor cortex which is located in the frontal lobe of the brain. There are several research works related to movement-related (either voluntary or imagery) hemodynamics classifications for BCI applications.

The activation patterns of the voluntary and imagery movement-based stimuli are widely examined in [12-15]. These studies suggested that several areas in the motor cortex and some prefrontal cortex become active due to movement execution and imagination. Voluntary and imagery movement-related tasks were not classified by machine learning algorithms. In [16], the two-class problems of imagery left and right-hand wrists movement were classified with the Linear Discriminant Analysis (LDA) method. Three classes of BCI were studied in [17], with two classes being motor imagery tasks. Voluntary movement-related tasks of the left and right hand were classified in [18] from the fNIRS signals of optimally selected channels. Multiple motor imagery tasks (movements of the left hand, right hand, left foot, and right foot) were classified in [19]. In these works, authors classified either the voluntary or imagery movement-related fNIRS signals. To the best of our knowledge, no work classified fNIRS signals regarding both voluntary and imagery movement stimuli. This is a challenge for the researchers to find the voluntary and imagery movement related fNIRS signal, simultaneously, because the activation area of the voluntary and imagery movement by an organ is the same in the brain [13] and their activation strengths are alike. This is a challenge for signal classification at high classification accuracy that was considered to be solved in this work.

In this work, both voluntary and imagery movement fNIRS signals were classified separately utilizing Linear Discriminant Analysis (LDA) and Support Vector Machines (SVM). We found satisfactory results for two class voluntary and two class motor imagery fNIRS signals. Additionally, we made it a four-class problem adding the voluntary and imagery fNIRS signals together and thereafter we classified the signal utilizing the same procedure applied with LDA and SVM. In this approach,

the classification accuracy was only 55-65%. This is a great barrier to implementing neuro-rehabilitate prosthetics where several events occur and the classification must be accurate and precise. To improve the classification accuracy for such a problem, we deployed a Convolutional Neural Network (CNN) which has an automatic feature extraction capability. Since the fNIRS signals are of multiple channels, the time series data of the change in the concentration of oxidized hemoglobin (HbO<sub>2</sub>) and deoxidized hemoglobin (dHb) are used to prepare two-dimensional data. These data were used to prepare topographic images of the hemodynamic activations and are fed to the proposed CNN structure. Our proposed CNN method can classify the 4-class fNIRS signal with 86.14% (on average) accuracy which is a significant improvement. Therefore, the contribution of this research work can be summarized as:

- Developing a shallow deep neural network to classify multiple class fNIRS signals with high accuracy.
- Proposing a method for effective BCI for same limb voluntary-imagery fNIRS signal classification in subject dependent and independent approach.

## II. MATERIALS AND METHODS

### A. Dataset

The dataset used in this research is available in [20], and was collected with permission from the authors. According to the description given in [20], the participants were healthy. In their experiment, four types of tasks were performed by the subjects: left hand (LH) movement, right-hand (RH) movement, imagery left-hand (iLH) movement, and imagery right-hand (iRH) movement. Therefore, the subjects performed two voluntaries and two imagery hand movement tasks in different sessions. In each trial, a subject performed a 10-second task of two different movements with 20 seconds of rest after each task. At first, 20 seconds passed at the resting condition to correct the baseline values of the data. A 10-second task followed. This task might be LH or iLH. This was followed by another 20-second resting period, which was followed by another 10 second task which was either RH or iRH. This trial was repeatedly performed. Each subject performed 5 trials in each session. As a whole, sixteen (16) sessions (8 voluntary and 8 imagery) were performed by every participant in a total of 40 trials of each task. Eventually, 40 trials of 4-class data were acquired from every subject. The fNIRS data were acquired using fNIR devices [21], which have 4 NIR sources and 10 detectors. The optode of this device covers 16 channels. The device provides a measure of continuous real-time concentration change in the values for HbO<sub>2</sub> and Hb. The Cognitive Optical Brain Imaging (COBI) studio software was used to log the fNIRS data in computer memory [22].

### B. Methods

In this section, all the data processing steps from signal acquisition to event classification for the performance test are explained. After designing the data acquisition protocol, data from prefrontal hemodynamics were collected. Then, in order to reduce dimensions, data compression using Principle Component Analysis (PCA) was applied. After that, the

baseline of fNIRS data was corrected. As a part of the pre-processing, these data were filtered. Then the data were separated into some sequential events and some prominent features were extracted. Using these features, classification accuracy was calculated. The main steps of the proposed data processing methods for the fNIRS data classification are presented briefly in Figure 1. The Figure is mainly focused on the conventional data classification technique. The steps are also described concisely with technical details in this subsection. Feature extraction and classification procedure by CNN are also discussed in order to clarify how this proposed method customized the CNN structure for achieving the objectives of the proposed method.

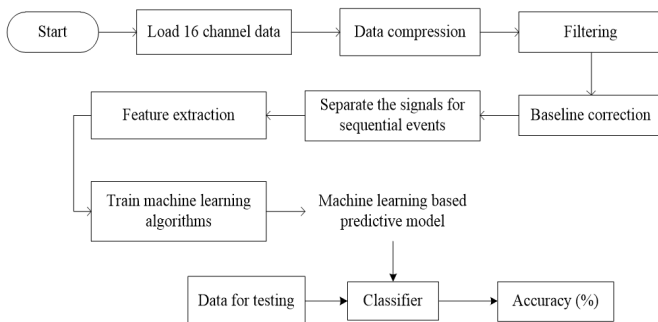


Fig. 1. Block diagram of the total signal processing steps to create a machine learning-based predictive model and the accuracy of the testing data.

### 1) Data Compression

Since the data were acquired with 16 channels, the processing could face the issue of high dimensionality. To check the actual dimensions, the data were transformed by PCA and it was found that the actual dimension of the data was 4 instead of 16. The result of PCA is shown in Figure 2 with a similar channel number of ilk dimension. The resulting 4 dimensions are termed as Left Lateral (LL: channel 1, 2, 3, 4), Left Medial (LM: channel 5, 6, 7, 8), Right Medial (RM: channel 9, 10, 11, 12), and Right Lateral (RL: 13, 14, 15, 16). The signals having the same dimension were averaged. Therefore, the 16-channel configuration becomes compressed from  $i \times 16$  to  $i \times 4$ . This compression helps reduce the feature dimension, which is very important for achieving high classification accuracy in the machine learning approach.

### 2) Filtering and Baseline Correction

Since fNIRS electrodes collect data from the human body, the signal is full of artifacts and noises. So, removing different types of noises is the first step of data processing. The fNIRS data can be affected by three types of noise [23]. These are motion artifacts, physiological signals, such as heart rate and respiration, and instrument and environment-related noises. Motion artifacts occur due to head movement and it results in fNIRS detectors shifting and losing contact with the skin exposing them to ambient light or light emitted directly from the fNIRS source. These types of motion artifacts can be easily recognized because they cause sudden, large spikes in the raw fNIRS data. Rapid head movements can cause the blood to move toward or away from the area that is being monitored,

rapidly increasing or decreasing blood volume. As the dynamics of this type of motion artifacts are slower than LED pop, they can be confused with the actual hemodynamic response due to brain activation. Physiological signals such as heart rate (over 0.5Hz) and respiration (over 0.2Hz) are at higher frequency ranges than hemodynamic responses, thus they should also be eliminated. So the raw fNIRS signals were filtered by a Savitzky-Golay filter of the 3rd order with 21 frame length (equivalent to 0.1Hz cut-off FIR low pass filter in 2Hz fNIRS signal) [10]. The raw noisy and filtered data of fNIRS are shown in Figure 3. Then, the data were separated in each trial. Every trial of the fNIRS data was corrected by subtracting the baseline from the original signal. The baseline was calculated by averaging the data of the first task.

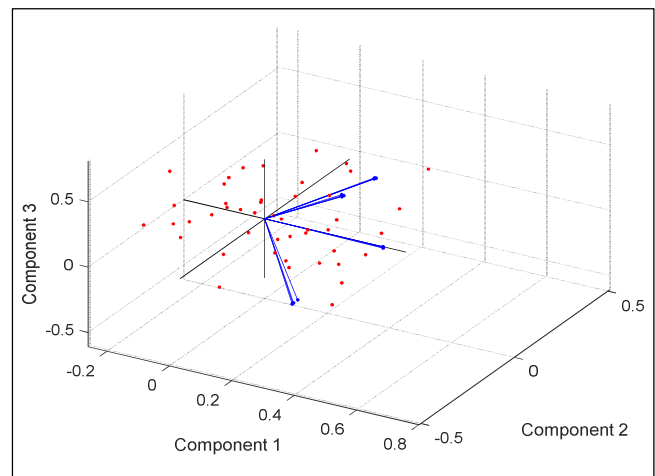


Fig. 2. Principle component 1 vs. component 2 presents the actual signal dimensions in eigenspace.

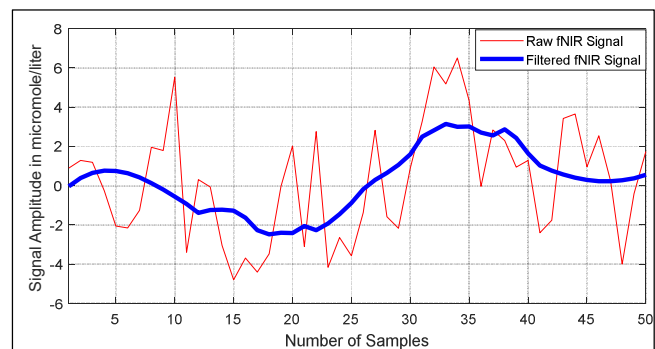


Fig. 3. The raw fNIRS signal with physiological artifacts and the filtered signal after the Savitzky-Golay filtering technique.

### 3) Feature Extraction

When the input data are too large to be processed and are suspected to be redundant, then they can be transformed into a reduced set of features. Analyzing a large number of input variables requires a large amount of memory and computation power. It also over-fits the classification algorithms. The selected features are expected to contain the relevant information from the input data so that the desired task can be performed by using this reduced representation instead of the

complete initial data. In this study, mean, slope, standard deviation, and skewness were extracted as the dominant features. Since the fNIRS signal does not exhibit complexity like EEG, MEG, or fMRI, simple time domain features are enough to represent the signal characteristics [23]. In this experiment, we have worked with the above features. Before training the machine learning-based network, all the values of the training features were normalized between 0 and 1.

$$\pi' = \frac{\pi - \pi_{\min}}{\pi_{\max} - \pi_{\min}} \quad (1)$$

where  $\pi'$  are the feature values that are rescaled between 0 and 1. On the other hand,  $\pi \in R^n$  are the actual values of the features. The maximum and minimum values of the features are presented as  $\pi_{\max}$  and  $\pi_{\min}$  respectively.

#### 4) Classification Methods

Classification is the process of predicting the class of given data points. Classes are sometimes called targets. Classification predictive modeling is an important task of approximating a mapping function from input variables to discrete output variables. A training process continues until the model achieves the desired level of accuracy on the training data for the SVM- and LDA-based predictive models. Since the machine learning models (SVM and LDA) gave lower accuracy in multiclass (4-class classification) problems, CNN (a deep neural network) is applied.

#### C. Deep Neural Network-based Classification

A deep neural network needs no extracted features because it extracts features from its own. A CNN is one of the best formats of deep neural networks. In this work, CNN is utilized for fNIRS data classification. Since the feature extraction and classification process are included in the CNN structure, it is very important to prepare the input layer and output layer of CNN. The fNIRS data preparation to run the CNN and the structure of the proposed CNN layers are described briefly below.

##### 1) Input Preparation

CNN is applied when the inputs are images or a two-dimensional matrix. When the computer sees an image, it will see an array of pixel values depending on the dimension of images. The image dimension is  $32 \times 32$ . So it will see an array of  $32 \times 32 \times 3$  numbers for RGB values and  $32 \times 32 \times 1$  for grayscale images. Each of these numbers is given a value from 0 to 255 that describes the pixel intensity at that point. CNN consists of convolutional, nonlinear, pooling, and fully connected layers. In convolutional layers, a convolutional filter whose width is equal to the dimension of the input and kernel size is convolved with the input data. To build the feature map, the output of the convolutional layer is converted by an activation function similar to ANNs'. After each convolutional layer, additional subsampling operations such as max-pooling and softmax are performed to enhance the performance [24-25]. As with ANNs, hyper-parameters such as learning rate, batch size, and the number of epochs should be investigated for the CNN to improve its classification performance.

##### 2) Structure of the CNN Layers

In this research, at first any two events: motor imagery hand movement or motor execution hand movements were classified by two shallow neural networks (SVM and LDA), with satisfactory accuracy. But when the 4-event classification was performed, the accuracy became very low, which means shallow neural networks like SVM and LDA cannot be utilized for more than 2-class events. To improve this result, the CNN algorithm is proposed. A general structure of a CNN is given in Figure 4 including its main layers.

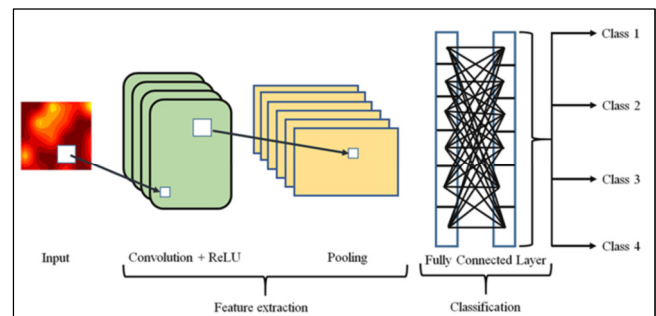


Fig. 4. Layers (convolutional, ReLU, pooling, and fully connected) of a CNN.

Deep learning is a class of machine learning algorithms that uses a cascade of multiple layers of nonlinear processing units for feature extraction and transformation. A CNN is highly capable of automatically learning appropriate features from the input data by optimizing the weight parameters of each filter, using forward and backward propagation to minimize classification errors.

##### a) Convolution Layer

The convolution layer is the first layer to extract features from an input image (as given in Figure 4). Convolution preserves the relationship between pixels by learning the image features using small squares of input data. It is a mathematical operation that takes two inputs, the image matrix and a filter or kernel. Consider the dimension of an image matrix is  $h \times w \times d$  and the filter's is  $f_h \times f_w \times d$ . So, the output of the matrix dimension is  $(h - f_h + 1) \times (w - f_w + 1) \times 1$ .

A very important note is that the depth of the filter should be the same as the depth of the input image. So for a  $5 \times 5 \times 3$  image, the dimension of the filter is  $5 \times 5 \times 3$ . Starting from the first position of the input image, the filter is sliding or convolving around the input image, it is multiplying the values in the filter with the original pixel values of the original image. The method used in this work to prepare the input images from the data ( $\text{HbO}_2$  and  $\text{Hb}$ ) is illustrated in Figure 5. The way convolutional filters worked on the images is shown in Figure 6. This multiplication is all summed up and a single number will be found. It should be remembered that this single number is only for when the filter is on the starting corner of the input image. This process is repeatedly performed for every location of the image.

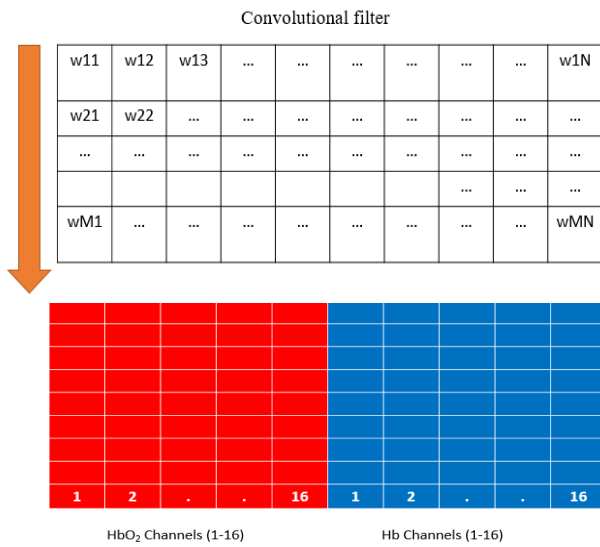


Fig. 5. The input data consisting of the concentration changes of HbO<sub>2</sub> (red) and Hb (blue) overall channels. A convolutional filter runs through the input data along the vertical axis.

b) ReLU Layer

ReLU (Rectified Linear Unit) layer induces nonlinearity in the values of the incoming layer. The ReLU function only passes the values  $x$  which are greater than zero:

$$f(x) = \begin{cases} x & \text{if } x > 0 \\ 0 & \text{if } x \leq 0 \end{cases} \quad (2)$$

Other functions are also used to increase nonlinearity, for example  $f(x) = \tanh(x)$ ,  $f(x) = |\tanh(x)|$ , and the sigmoid function  $f(x) = \frac{1}{1+e^x}$ . ReLU is often preferred to other functions because it trains the neural network several times faster without a significant penalty to generalization accuracy.

c) Pooling Layer

This layer reduces the number of parameters if the images are too large. Spatial pooling is also called downsampling and reduces the dimensionality of each map, but retains the important information. Spatial pooling can be of different types: Max pooling, average pooling, and sum pooling. In this work, the max pooling layer is used.

d) Fully Connected Layer

This layer takes the output of the convolution, ReLU, and pooling layers as input. With the fully connected layers, we combine these features to create a model. Finally, we have an activation function such as softmax or sigmoid to classify the outputs.

e) Cross Validation

$k$ -fold cross-validation is used to estimate the classification performance of the predictive model. The first step in this process is to divide the data into  $k$  folds, where each fold contains an identical amount of input data. One fold is used as a test dataset, while the remaining folds are used as training sets. Afterward, a classification procedure is applied to the

selected test and training sets. This process is performed for each of the  $k$  folds. In this study, 5-fold cross-validation was performed. The parameters of different layers and the structure of the proposed CNN are summarized in Table I.

TABLE I. CNN LAYER PARAMETERS

Parameters	Value
Matrix input layer	384×384
Convolution layer 1	2, 8
Max-pooling layer 1	2 (pool size)
Convolution layer 2	4, 16
Max-pooling layer 2	2 (pool size)
Fully connected layer	4
Learning rate	0.01
Epoch	15
Validation frequency	3

III. RESULTS AND DISCUSSION

The activation due to imagery movement planning occurs in the prefrontal cortex which can be measured by the increased concentration of HbO<sub>2</sub>. For the left-hand and right-hand imagery movement planning, the activation level is found to be increased in the concentration of HbO<sub>2</sub> in the right hemisphere and left hemisphere, respectively. Since 4 different portions are selected to observe the actual concentration change in HbO<sub>2</sub> of LH and RH movement planning. The variation of HbO<sub>2</sub> concentration in the LL, LM, RM, and RL portions of the prefrontal cortex due to planning movements of LH and RH of a randomly selected subject is presented in Figures 6 and 7.

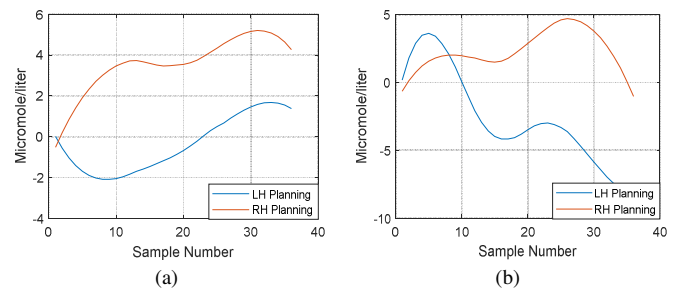


Fig. 6. Comparison of the concentration changes in HbO<sub>2</sub> between LH and RH movement planning in (a) LL and (b) LM portion of the prefrontal cortex.

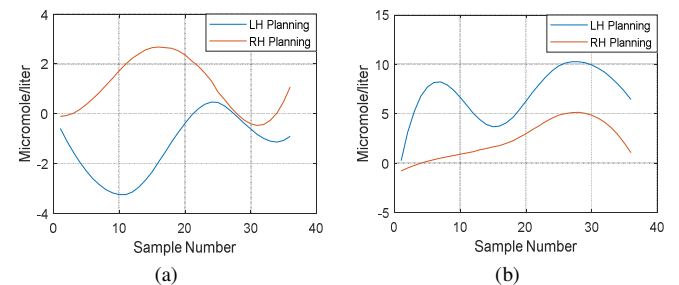


Fig. 7. Comparison of the concentration changes in HbO<sub>2</sub> between LH and RH movement planning in (a) RM and (b) RL portion of the prefrontal cortex.

It is easily observable from Figures 6 and 7 that all the proposed portions of the prefrontal cortex exhibit significant variations in the concentration of HbO<sub>2</sub>.

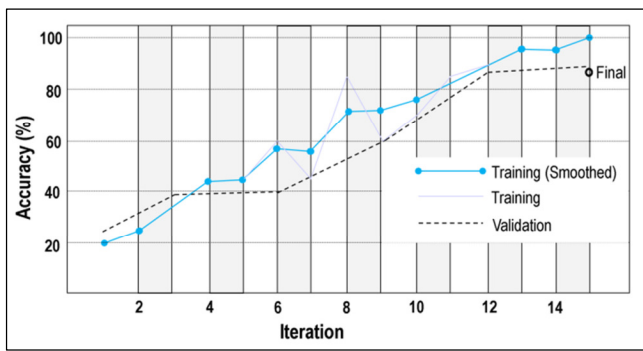


Fig. 8. Training and validation progress with loss reduction process in CNN.

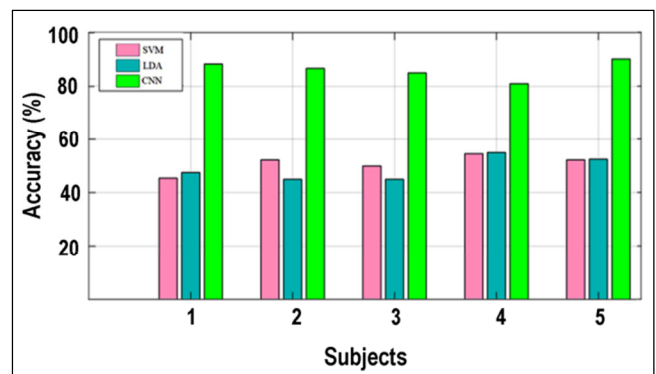


Fig. 9. Classification accuracy comparison of SVM, LDA, and CNN.

TABLE II. CLASSIFICATION ACCURACY OF LDA AND SVM FOR 2-CLASS AND 4-CLASS fNIRS SIGNAL

Sub	SVM classification accuracy (%)		LDA classification accuracy (%)		SVM 4-class classification accuracy (%)	LDA 4-class classification accuracy (%)
	LH vs RH	iLH vs iRH	LH vs RH	iLH vs iRH		
1	80	77.5	90	81.5	45.45	47.5
2	83.5	80	92.5	82	52.27	45
3	78	69.5	78	69.5	50	45
4	80	72	85	73.5	54.54	55
5	83.5	81.5	88.5	80	52.27	52.5

As a result, all these portions should have to be taken into account as a significant source to discriminate the imagery activities. Accordingly, features were extracted from the fNIR signals of LL, LM, RM, and RL. The features were used to train SVM and LDA separately to check the feature-dependent accuracy of the predictive model. Several time domain features like variance, total summation, and kurtosis did not return good classification accuracy except mean and slope. The classification accuracies for two classes by SVM and LDA were satisfactory. But for 4 classes, the classification accuracy was very low. The results are given in Table II. Therefore, CNN was applied in order to improve the classification accuracy for the 4-class problem.

The training progress of CNN is shown in Figure 8. Here, both training accuracy and loss are shown graphically for a randomly chosen subject. The classification accuracy of the applied CNN is presented in Figure 9 along with the results of SVM and LDA. From the results given in Figure 9, it was found that the classification accuracy of CNN for the 4-class fNIRS signal is way more satisfactory than the results of LDA and SVM.

IV. CONCLUSION

This research work investigates how CNN can enhance the classification accuracy with data of more than two classes when the SVM and LDA classification accuracy is very low. The results show that for iLH, iRH, LH, and RH on five subjects, the CNN-based scheme provides 86.24% (on average) accuracy, whereas, in the case of SVM and LDA, the average classification accuracy is 50.9% and 49%, respectively. In the case of subject-independent data, CNN shows 83.33% accuracy. This result revealed that CNN can lead to the practical development of a BCI system. Since classification accuracy is the most essential factor to design a practical BCI

device, we will try to explore further improvements in the accuracy of fNIRS-based BCI by implementing several deep learning-based algorithms. We can also try to merge some other modalities with fNIRS and check whether this process provides better accuracy or not.

ACKNOWLEDGMENT

The authors acknowledge the partial financial support provided by the Department of Biomedical Engineering, MIST, Dhaka-1216, Bangladesh.

REFERENCES

- [1] S. Ajami, A. Mahnam, and V. Abootalebi, "Development of a practical high frequency brain-computer interface based on steady-state visual evoked potentials using a single channel of EEG," *Biocybernetics and Biomedical Engineering*, vol. 38, no. 1, pp. 106-114, Jan. 2018, <https://doi.org/10.1016/j.bbe.2017.10.004>.
- [2] A. Rezeika, M. Benda, P. Stawicki, F. Gemblor, A. Saboor, and I. Volosyak, "Brain-Computer Interface Spellers: A Review," *Brain Sciences*, vol. 8, no. 4, Apr. 2018, Art. no. 57, <https://doi.org/10.3390/brainsci8040057>.
- [3] F. Cincotti *et al.*, "Non-invasive brain-computer interface system: Towards its application as assistive technology," *Brain Research Bulletin*, vol. 75, no. 6, pp. 796-803, Apr. 2008, <https://doi.org/10.1016/j.brainresbull.2008.01.007>.
- [4] K. D. Tzamourta *et al.*, "Evaluation of window size in classification of epileptic short-term EEG signals using a Brain Computer Interface software," *Engineering, Technology & Applied Science Research*, vol. 8, no. 4, pp. 3093-3097, Aug. 2018, <https://doi.org/10.48084/etasr.2031>.
- [5] "What Is MEG?" <http://web.mit.edu/kitmitmeg/whatis.html> (accessed Feb. 15, 2023).
- [6] H. Y. Kim, K. Seo, H. J. Jeon, U. Lee, and H. Lee, "Application of Functional Near-Infrared Spectroscopy to the Study of Brain Function in Humans and Animal Models," *Molecules and Cells*, vol. 40, no. 8, pp. 523-532, Aug. 2017, <https://doi.org/10.14348/molcells.2017.0153>.
- [7] Md. A. Rahman and M. Ahmad, "Identifying appropriate feature to distinguish between resting and active condition from FNIRS," in *3rd International Conference on Signal Processing and Integrated*

- Networks, Noida, India, Feb. 2016, pp. 671–675, <https://doi.org/10.1109/SPIN.2016.7566781>.
- [8] N. Naseer and K.-S. Hong, "fNIRS-based brain-computer interfaces: a review," *Frontiers in Human Neuroscience*, vol. 9, 2015, Art. no. 3, <https://doi.org/10.3389/fnhum.2015.00003>.
- [9] S. N. Abdulkader, A. Atia, and M.-S. M. Mostafa, "Brain computer interfacing: Applications and challenges," *Egyptian Informatics Journal*, vol. 16, no. 2, pp. 213–230, Jul. 2015, <https://doi.org/10.1016/j.eij.2015.06.002>.
- [10] Md. A. Rahman, M. A. Rashid, and M. Ahmad, "Selecting the optimal conditions of Savitzky–Golay filter for fNIRS signal," *Biocybernetics and Biomedical Engineering*, vol. 39, no. 3, pp. 624–637, Jul. 2019, <https://doi.org/10.1016/j.bbe.2019.06.004>.
- [11] K.-S. Hong, M. J. Khan, and M. J. Hong, "Feature Extraction and Classification Methods for Hybrid fNIRS-EEG Brain-Computer Interfaces," *Frontiers in Human Neuroscience*, vol. 12, 2018, Art. no. 246, <https://doi.org/10.3389/fnhum.2018.00246>.
- [12] T. Hanakawa, I. Immisch, K. Toma, M. A. Dimyan, P. Van Gelderen, and M. Hallett, "Functional Properties of Brain Areas Associated With Motor Execution and Imagery," *Journal of Neurophysiology*, vol. 89, no. 2, pp. 989–1002, Feb. 2003, <https://doi.org/10.1152/jn.00132.2002>.
- [13] S. C. Wriessnegger, J. Kurzman, and C. Neuper, "Spatio-temporal differences in brain oxygenation between movement execution and imagery: A multichannel near-infrared spectroscopy study," *International Journal of Psychophysiology*, vol. 67, no. 1, pp. 54–63, Jan. 2008, <https://doi.org/10.1016/j.ijpsycho.2007.10.004>.
- [14] A. M. Batula, J. A. Mark, Y. E. Kim, and H. Ayaz, "Comparison of Brain Activation during Motor Imagery and Motor Movement Using fNIRS," *Computational Intelligence and Neuroscience*, vol. 2017, May 2017, Art. no. e5491296, <https://doi.org/10.1155/2017/5491296>.
- [15] S. M. S. Galib, S. Md. R. Islam, and Md. A. Rahman, "A multiple linear regression model approach for two-class fNIR data classification," *Iran Journal of Computer Science*, vol. 4, no. 1, pp. 45–58, Mar. 2021, <https://doi.org/10.1007/s42044-020-00064-0>.
- [16] N. Naseer and K.-S. Hong, "Classification of functional near-infrared spectroscopy signals corresponding to the right- and left-wrist motor imagery for development of a brain–computer interface," *Neuroscience Letters*, vol. 553, pp. 84–89, Oct. 2013, <https://doi.org/10.1016/j.neulet.2013.08.021>.
- [17] K.-S. Hong, N. Naseer, and Y.-H. Kim, "Classification of prefrontal and motor cortex signals for three-class fNIRS–BCI," *Neuroscience Letters*, vol. 587, pp. 87–92, Feb. 2015, <https://doi.org/10.1016/j.neulet.2014.12.029>.
- [18] A. Janani and M. Sasikala, "Evaluation of classification performance of functional near infrared spectroscopy signals during movement execution for developing a brain–computer interface application using optimal channels," *Journal of Near Infrared Spectroscopy*, vol. 26, no. 4, pp. 209–221, Aug. 2018, <https://doi.org/10.1177/0967033518787331>.
- [19] A. M. Batula, H. Ayaz, and Y. E. Kim, "Evaluating a four-class motor-imagery-based optical brain-computer interface," in *36th Annual International Conference of the IEEE Engineering in Medicine and Biology Society*, Chicago, IL, USA, Aug. 2014, pp. 2000–2003, <https://doi.org/10.1109/EMBC.2014.6944007>.
- [20] Md. A. Rahman, M. S. Uddin, and M. Ahmad, "Modeling and classification of voluntary and imagery movements for brain–computer interface from fNIR and EEG signals through convolutional neural network," *Health Information Science and Systems*, vol. 7, no. 1, Oct. 2019, Art. no. 22, <https://doi.org/10.1007/s13755-019-0081-5>.
- [21] "fnir-devices-technology.pdf." Accessed: Feb. 15, 2023. [Online]. Available: <https://www.biopac.com/wp-content/uploads/fnir-devices-technology.pdf>.
- [22] "COBI fNIR Imager software | BIOPAC," *BIOPAC Systems, Inc.* <https://www.biopac.com/upgrade/cobi-fnir-imager-software/>.
- [23] Md. A. Rahman, M. A. Rashid, M. Ahmad, A. Kuwana, and H. Kobayashi, "Activation Modeling and Classification of Voluntary and Imagery Movements From the Prefrontal fNIRS Signals," *IEEE Access*, vol. 8, pp. 218215–218233, 2020, <https://doi.org/10.1109/ACCESS.2020.3042249>.
- [24] N. C. Kundur and P. B. Mallikarjuna, "Deep Convolutional Neural Network Architecture for Plant Seedling Classification," *Engineering, Technology & Applied Science Research*, vol. 12, no. 6, pp. 9464–9470, Dec. 2022, <https://doi.org/10.48084/etasr.5282>.
- [25] S. Nuanmeesri, "A Hybrid Deep Learning and Optimized Machine Learning Approach for Rose Leaf Disease Classification," *Engineering, Technology & Applied Science Research*, vol. 11, no. 5, pp. 7678–7683, Oct. 2021, <https://doi.org/10.48084/etasr.4455>.